

Influence of Reaction Time on Growth Behaviours of Mg-Al LDH Films

WU Liang^{1,2}, CHEN Jing¹, ZHANG Sheng¹, TANG Ai-tao^{1,2},
YANG Dan-ni³, ZHANG Gen¹, LIU Lei¹, PAN Fu-sheng^{1,2}

(1. Chongqing University, Chongqing 400044, China; 2. National Engineering Research Center for Magnesium Alloys, Chongqing 400044, China; 3. Harbin Institute of Technology, Harbin 150001, China)

ABSTRACT: Mg-Al LDH film was fabricated on anodized magnesium alloy AZ31 by in-situ growth method. The characteristics of the film were investigated by X-ray diffraction (XRD), Fourier transform infrared (FT-IR), scanning electron microscopy (SEM) observation and electrochemical tests. The results showed that the crystallinity of LDH film was increased with reaction time. When the reaction time was more than 12 h, the LDH film had complete crystal layered structure. The anodic oxide film was sealed basically by the growth of LDH nanosheets after 6 h reaction. The corrosion resistance of the films became better with the increasing of reaction time. However, after 12 h reaction, the corrosion resistance of the film decreased. The formation behavior of the Mg-Al LDH film was proposed. That the competitive growth of LDH grains, which contains dissolution and re-crystallization, was proposed to explain the change of the growth and corrosion resistance of the Mg-Al LDH film.

KEY WORDS: magnesium alloy; corrosion resistance; in-situ growth; layered double hydroxide (LDH); reaction time

中图分类号: TG174.44 文献标识码: A 文章编号: 1001-3660(2019)03-0019-08

DOI: 10.16490/j.cnki.issn.1001-3660.2019.03.003

Introduction

Magnesium and its alloy have attracted interest for a broad area of industrial applications, such as automotive, aerospace and portable electronic devices^[1-3], because of their superior strength/weight ratio, dimensional stability and light weight^[4]. But their application scope is limited by their poor corrosion resistance. Therefore, an improvement in corrosion resistance is of critical importance for magnesium alloys. Up to now, various approaches, including anodizing, chemical surface conversion^[5], organic polymer coating^[6], vapor deposition^[7], had been proposed to improve the corrosion resistance of magnesium-based alloys. Anodizing is used as an industrial technology for surface protection of light metals to improve corrosion resistance by forming an anodic oxide layer, which has been successfully used over many decades^[8-9]. However, for industrial

applications, the corrosion resistance of anodic oxide films is not sufficient, because the films are normally porous and contain many cracks and defects^[10]. In this study, we adopted a novel method by forming layered double hydroxides (LDHs) on anodic oxide layer, instead of the conventional boiling water sealing of pores. This method combines anodic oxide films and chemical conversion films, providing longer protection for magnesium alloys substrate.

Layered double hydroxides (LDHs) is a kind of typical two-dimensional layered nanomaterial. The general formula is $[M^{2+}_{1-x}M^{3+}_x(OH)_2]^{x+}(A^{n-})_{x/n} \cdot mH_2O$, where M^{2+} and M^{3+} are metal cations such as Mg^{2+} and Al^{3+} , that occupy octahedral sites in the hydroxide layers, A^{n-} is an exchangeable anion, and x is the molar ratio of $M^{3+}/(M^{2+}+M^{3+})$ ^[11-13]. In the case of Mg-Al LDHs, the atomic structure consists of brucite-like octahedral layers and these layers are charged positively by the

收稿日期: 2018-12-10; 修订日期: 2019-01-31

Received: 2018-12-10; Revised: 2019-01-31

基金项目: 国家自然科学基金 (51701029, 51531002, 51474043); 中国国家重点研究发展计划 (2016YFB0301100); 重庆市基础研究与前沿技术研究计划 (cstc2016jcyjA0388, cstc2017jcyjBX0040); 中国博士后科学基金资助项目 (2017M620410, 2018T110942); 重庆博士后科研基金 (Xm2017010); 中央高校基础研究经费 (2018CDGFCL005)

Fund: Supported by the National Natural Science Foundation of China (51701029, 51531002, 51474043), the National Key Research and Development Program of China (2016YFB0301100), the Chongqing Research Program of Basic Research and Frontier Technology (cstc2016jcyjA0388, cstc2017jcyjBX0040), China Postdoctoral Science Foundation Funded Project (2017M620410, 2018T110942), the Chongqing Postdoctoral Scientific Research Foundation (Xm2017010), the Fundamental Research Funds for the Central Universities (2018CDGFCL005)

作者简介: 吴量 (1985—), 男, 博士, 副教授, 主要研究方向为镁、铝、钛等合金的阳极氧化相关技术。邮箱: wuliang@cqu.edu.cn

Biography: WU Liang (1985—), Male, Doctor, Associate professor, research focus: anodizing and related technologies of magnesium, aluminum, titanium and other alloys. E-mail: wuliang@cqu.edu.cn

replacement of some Mg^{2+} with Al^{3+} ions. The ion exchange capacity of LDH improve its corrosion resistance^[4,14]. In general, the reported preparation methods of LDH structured thin film were solvent evaporation method^[15], electrophoresis deposition (EPD)^[16], coprecipitation^[11,17], spin-coating^[18-19], layer-by-layer assembly (LBL)^[19-20], in-situ growth^[21] and so on. Compared with other method, the chemical bonding generated by in-situ method gives rise to a strong adhesion force between the films and the substrate. These have a great meaning on maintaining film properties and polarizing practical application^[21].

In previous studies^[17,22-23], LDHs was fabricated by adding the mixture solutions of divalent and trivalent metal salts at the selected ratio into a reactor containing the desired interlayer anion. There were also researchers who only added a metal salt to the synthesis of LDHs^[24-25]. For instance, Ishizaki et al. used a divalent metal salt aqueous solution as a steam source to prepare LDHs on the surface of aluminium alloy. Also, some researchers^[26-27] firstly anodized aluminium alloy substrate and sealed pores of anodic oxide films on the substrate by the fabrication of LDHs, using the single component of alumina as internal source of trivalent cations. In order to synthesize LDHs, a kind of divalent metal salt was introduced. In a word, the majority of researchers at least introduced a kind of metal salt to fabricate LDHs, and few researchers just used anodic films as internal source of cations to synthesize LDHs.

Different from others, only one kind of trivalent cation Al^{3+} was used. Besides, the LDHs was fabricated on the surface of the anodic oxide film and the Mg^{2+} was got from the anodic oxide film. In this study, a novel approach was explored using anodic oxide layer as internal source of cations to fabricate LDHs on common commercial magnesium alloy AZ31.

The density of LDH film has a great impact on its corrosion resistance, and according to crystal growth kinetics, reaction time impacts the crystallinity and the grain size, then impacts the density. Kamiyama et al. demonstrated that the film coated for 7 h exhibited the lowest corrosion current density^[4]. Zhang compared the corrosion resistance of the Mg-Al LDH film coated for 24 h and 48 h, finding the latter was better^[28]. In this study, the Mg-Al LDH films were prepared on AZ31 Mg-Al alloy by using in-situ growth method. The effects of reaction time on morphological, structural and chemical properties of the LDH films were studied by SEM, XRD and FT-IR, respectively. The corrosion resistance of the Mg-Al LDH films was investigated by polarization curve and EIS. Finally, the relationships between the growth of Mg-Al-LDH film and reaction time were concluded. The formation behavior of the LDH film was proposed and the main content was the competitive growth of LDH grains.

1 Experimental procedures

1.1 Anodizing process

The substrate was common commercial cast magnesium

alloy AZ31 (the nominal compositions: Al 2.5wt.%~3.5wt.%, Zn 0.6wt.%~1.3 wt.%, Mn 0.2wt.%~1wt.%, Ca 0.04wt.%, Si 0.1wt.%, Cu 0.05wt.%, and balanced Mg). Firstly, the alloy sheets were ground to 2000 grit SiC paper, then anodized in mixture solutions of 7.14 g/L NaOH and 4 g/L $NaAlO_2$ for 30 min with applied voltage of 20 V. Finally, ultrasonically cleaned in ethyl alcohol for 5 min and dried under a steam of air.

1.2 Fabrication of Mg-Al LDH film

Firstly, the mixed solution of 0.05 mol/L $Al(NO_3)_3 \cdot nH_2O$ and 0.3 mol/L NH_4NO_3 was prepared. Then the pH of the mixed solution was adjusted to 10.7. Next, anodized samples were soaked in mixed solution. After this, they were putted in autoclave, reacting closing in constant temperature in drying oven for 1 h, 3 h, 6 h, 12 h, 24 h. Finally, the as-prepared samples were washed with deionized water and dried under a steam of air.

1.3 Characterization

The morphologies of the surface of the LDH films were observed with a field-emission scanning electronic microscope (FE-SEM, JSM-7800F, JEOL, Japan) and the chemical composition was investigated using energy dispersive spectrum (EDS, INCA, Energy 350 Oxford, UK). The structures of the LDH films were determined using an X-ray diffractometer (XRD, D/Max 2500X Rigaku, Japan) at a glancing angle of 1.5° using Cu target ($\lambda=0.154$ nm) with 40 kV and 150 mA radiation. Fourier transform infrared (FT-IR, Nicolet IS5 Thermo Scientific, USA) spectra were obtained in the range of $4000\sim 400$ cm^{-1} .

Potentiodynamic polarization curves and electrochemical impedance spectra (EIS) were obtained in a cell with 3.5wt.% NaCl solution using CHI660 CH and CIMPS-2 Zahner, respectively. A classical three-electrode system was used with the sample as the working electrode (1 cm^2), a saturated calomel electrode (SCE) as the reference electrode, and a platinum plate as the counter electrode. The Potentiodynamic polarization curves were recorded with a sweep rate of 2 mV/s. EIS measurements were performed from 10 mHz to 100 kHz.

2 Results and discussion

2.1 Characterisation of Mg-Al LDH films formed at different reaction time

Fig.1 presents typical SEM micrographs of samples formed at different reaction time. As showed in Fig.1a, the reaction time greatly impacts grain size and density of Mg-Al LDH films. For the films reacted for 1 h, only under the higher magnification (Fig.1b), some tiny grains arranging on the surface of the substrate randomly were found. When the reaction time was 3 h (Fig.1d), there were fine grains around the hole. When the reaction time was 6 h (Fig.1e,f), the grain size changed obviously. These suggested that in this stage, the grain grew along three axis at the same time. It was seen that the diameter of holes in anodic oxide film decreased. After 6 h' reaction, the hole of anodic oxide

film was closed basically. When the reaction time was less than 12 h, the thickness and density of the films increased with the reaction time extending. After 12 h's reaction, the density of the LDH film decreased a little.

The pores of the anodic oxide film had been completely sealed by Mg-Al LDH films after 12 h' reaction. And this could be attributed to the size of the LDH grains increased with reaction time.

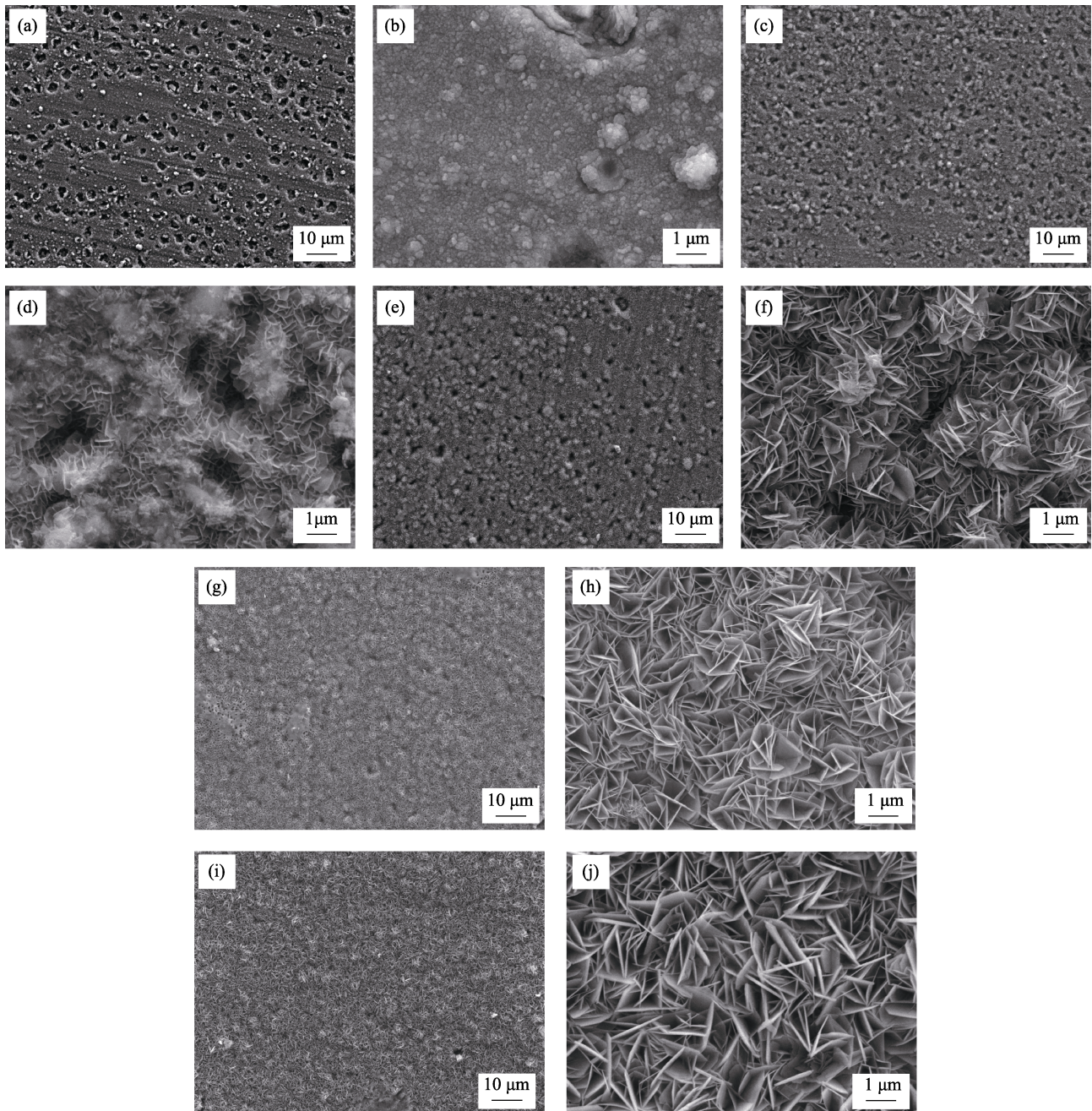


Fig.1 SEM surface morphologies of the LDH films in different reaction time

XRD patterns of the LDH films formed in different reaction time are shown in Fig.2. Two weak peaks were observed at approximately 11° and 22° (denoted as open triangle), which were associated with the (003) and (006) planes of hydrotalcite-like layered structure of Mg-Al LDH^[29]. When the reaction time was 1h, there was no obvious characteristic peak at 10° and only weak characteristic peak existed next to 20° . But for the samples reacted for 3 h, the characteristic peak in 10°

could be found obviously. The (003) and (006) characteristic peaks corresponding to the samples reacted for 6 h were obvious. The LDH film whose reaction time was 12 hours had good crystallinity, and this was mean to be that the product had complete layered structure and good crystal structure. Lengthening the reaction time made the LDH film had a better crystallinity. The LDH film crystallizing completely needing approximately 12 h.

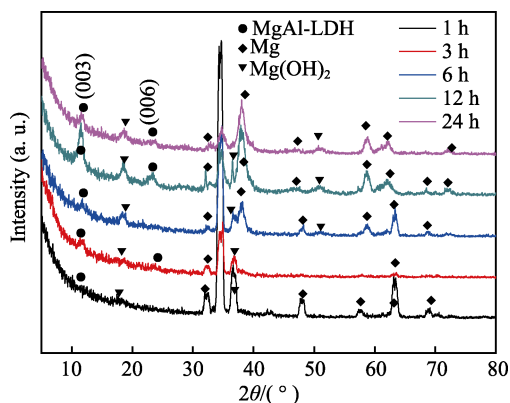


Fig.2 XRD patterns of the LDH films gained by different reaction time

Fig.3 displays the FT-IR spectrum of LDH in different reaction time. As observed in FT-IR spectra, the sharp peak at 3695 cm^{-1} could be attributed to the H—O—H stretching vibration. The absorption peaks at 3450 cm^{-1} and 1640 cm^{-1} corresponded to the O—H symmetric contraction and bending vibration of water molecules, respectively. This could attribute to the presence of the surface absorption water and interlayer water^[30]. The obvious broad band absorption bands at 3405 cm^{-1} were derived from the hydrogen bond between Hydroxyl metal functional groups and water molecule. The bands in the range of $444\sim 770\text{ cm}^{-1}$ are attributed to metal-oxygen-metal stretching^[31]. The asymmetric expansion peak of intercalated NO_3^- was about at 1350 cm^{-1} , which indicated that there were a few intercalated NO_3^- anions in the LDH samples. The increase in the absorption peak intensity indicated the increase in the existence amounts of the Mg-Al LDH, the interlayered anions, and the interlayered water in the film at longer time. The results was in good agreement with the analysis in XRD patterns. Lots of nucleation generated on the surface grew into LDH nanosheets with complete crystal structure gradually, and the crystallinity of LDH film increased. Finally, the anodic oxide film was sealed by the LDH nanosheets.

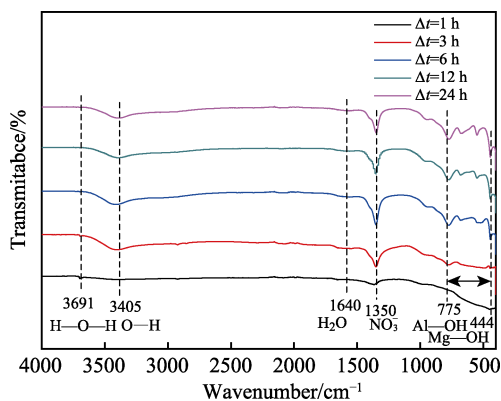


Fig.3 FT-IR spectrum of LDH in different reaction time

2.2 Corrosion resistance of LDH films formed at different reaction time

In order to evaluate the corrosion resistance of the

film, Tafel polarization measurements on specimens of the LDH film prepared at different reaction time after 0.5 hour immersion under 3.5wt.% NaCl solution are depicted in Fig.4. Table 1 lists the corrosion potentials (E_{corr}) and corrosion current density (J_{corr}) of Mg-Al-LDH samples prepared in different reaction time.

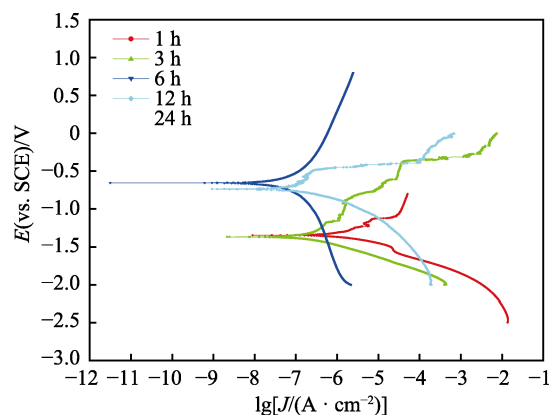


Fig.4 Tafel polarization curves in 3.5wt.% NaCl solution of the LDH films on magnesium alloy with different reaction time

Tab.1 Corrosion potential (E_{corr}) and corrosion current density (J_{corr}) of the samples

Reaction time/h	Test solution	E_{corr} (vs. SCE)/V	$J_{\text{corr}}/(\mu\text{A}\cdot\text{cm}^{-2})$
1	3.5wt.%NaCl	-1.370	0.8824
3	3.5wt.%NaCl	-1.345	0.6438
6	3.5wt.%NaCl	-1.341	0.1807
12	3.5wt.%NaCl	-0.6432	0.022 36
24	3.5wt.%NaCl	-0.7127	0.1077

E_{corr} of the LDH film in 1 h, 3 h, 6 h, 12 h and 24 h were -1.370 V(vs. SCE) , -1.345 V(vs. SCE) , -1.341 V(vs. SCE) , $-0.6432\text{ V(vs. SCE)}$ and $-0.7127\text{ V(vs. SCE)}$, respectively. From 1 h to 12 h, that the corrosion potential increases in turn showed that as the reaction time extending, the corrosion resistance of the films increased, and the degree of closure of anodic oxidation cavity improved, which blocked the matrix and the corrosive medium effectively. Besides, compared with the sample reacted for 12 h, the corrosion potential and corrosion current density of the LDH film gained by 24 h' reaction rose and fell respectively. The reasonable explanations for the above results were the decrease of the density of the LDH film. There were existing the competitive growth of LDH grains: tiny LDH grains dissolved, and bigger LDH grains continued to grow. The large LDH grains could not cover the anodic oxide film completely.

In order to further provide the information on the corrosion inhibition effect of the LDH films, EIS measurements on specimens after 0.5 hour immersion under 3.5wt.% NaCl solution are depicted in Fig.5. The Bode plots and the Nyquist plots of samples are presented in Fig.5a and Fig.5b, respectively. Its equivalent circuit diagram is also shown in Fig.5.

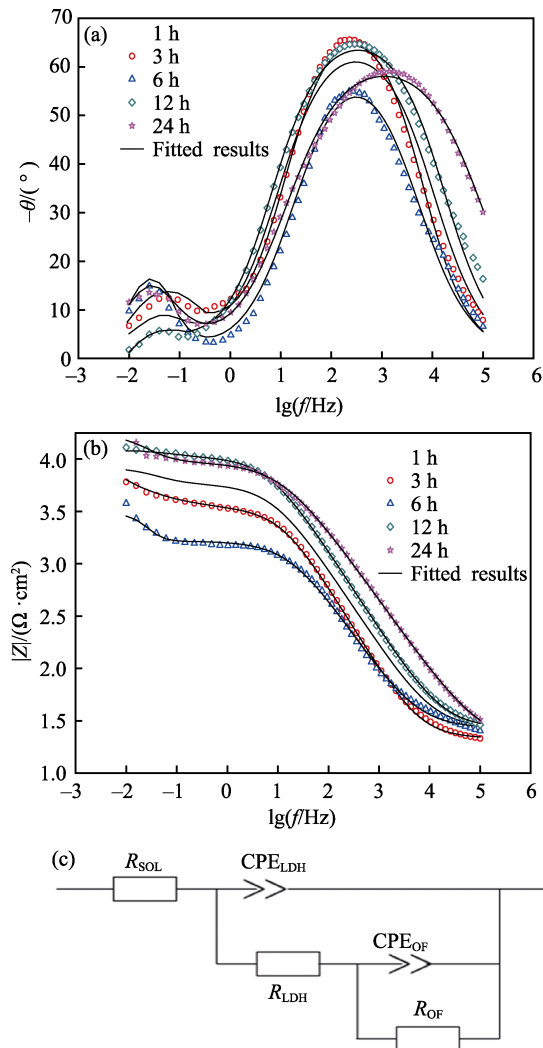


Fig.5 Bode diagrams (a, b) and the equivalent circuit (c) for LDH films in different reaction time immersed in 3.5 wt.% NaCl solution

The Frequency-Phase (frequency-phase angle) Bode diagram showed that the Mg-Al LDH layer, which was grown on the anode of magnesium oxide, had three time constants. In general, high frequency time constant corresponds to a loose outer layer structure of the composite films, while the time constant at low frequency could be ascribed to an inner compact layer structure^[32]. The LDH film is relatively loose and coarse from the previous SEM diagram. There is a significant difference between the LDH film layer and the anode magnesium oxide layer whose bottom has a high relative density. And this corresponds to the impedance difference between high frequency and intermediate frequency. At low frequency, the higher the Z value is, the better corrosion resistance of the material is. After the analysis, the equivalent circuit diagram of Fig.5 includes the following components: the R_{SOL} in the equivalent circuit diagram is the solution resistance; the C_{LDH} and R_{LDH} were the capacitance and resistance of the LDH films respectively; the C_{OF} and R_{OF} are the capacitance and resistance of the anode layer of magnesium oxide. Similarly, to reflect the heterogeneity of components, the pure capacitance C is replaced by the

constant phase element (CPE), and the relationship is $CPE=[C(j\omega)\alpha]^{-1}$. Capacitance characteristic of C is related to the α here. Usually, when $\alpha=1$, the constant phase element is the pure capacitance; when the $\alpha=0$, the constant phase element is the pure resistance.

The electrochemical impedance for anodized substrate coated with LDH films is given by Eq.1:

$$Z=R_{SOL}+\frac{1}{\frac{1}{Z_{LDH}}+\frac{1}{R_{LDH}+\frac{1}{\frac{1}{R_{OF}}+\frac{1}{Z_{OF}}}}} \quad (1)$$

Where, Z_{OF} represents the admittance of the constant-phase element of capacitance of the anodic oxide film. Constant phase element (CPE) is applied in place of a capacitor to compensate the non-homogeneity in the system, which is defined by two values, Q and n in Eq. 2:

$$Z=[Q(j\omega)^n]^{-1} \quad (2)$$

Where, the constant Q is the magnitude of CPE, and n is the empirical exponent of CPE, $0<n<1$. If $n=1$, Q is the pure capacitance; if $n=0$, Q is the pure resistance^[28].

The electrochemical impedance for the anodized substrate coated with LDH films are calculated and exhibited by Eq.3:

$$Z=R_{SOL}+\frac{1}{(j\omega)^n Q_{LDH}+\frac{1}{R_{LDH}+\frac{1}{R_{OF}+(j\omega)^n Q_{OF}}}} \quad (3)$$

According to Eq.3, the impedance of tested sample increases with the increase of resistance (R_{LDH} , R_{OF}) and the decrease of the capacitance (Q_{OF} , Q_{LDH}). Generally, a larger impedance corresponds to better anti-corrosion performance of the LDH films.

According to the fitting data in Table 2, the LDH layer had a high value of α_{LDH} , but low C_{LDH} . This showed that the arrangement of LDH grains in the bottom was very close, and it led to a relatively high R_{LDH} . When the reaction time was 1 h, the numerical R_{LDH} was relatively small. It indicated that the surface only had a few small LDH grains and this was consistent with the microscopic photos. When the reaction time was up to 12 h, the value of C_{LDH} decreased greatly and the numerical α_{LDH} increased to 1. These results demonstrate that the impedance of the LDH-coated samples increases with prolonging reaction time, leading to the full crystallization of the LDH coating in accordance with the XRD results presented in Fig.2^[21]. This can be attributed to the growth of LDH grains and the pores of anodic film have been well covered. When the reaction time exceeded 12 h, the corrosion resistance of the LDH films decreased a lot. The results were consistent with the data in Tafel polarization measurements.

The LDH layer, which is based on the anodic oxide film, had a high value of R_{OF} . It showed that, in the process of the growth of LDH film, the prolonging of

the reaction time contributed to the growth of LDH film on the surface of anodic oxide film, thereby affecting the structure of porous anodic oxide film. Finally, the pores

in anodic oxide films would be closed gradually and the growth of LDH crystals was in a state of equilibrium. Other scholars have found similar phenomena^[33].

Tab.2 Fitting data of Bode plots and the Nyquist plots

Reaction time/h	$R_{SOL}/(\Omega \cdot \text{cm}^2)$	CPE_{LDH}		$R_{LDH}/(\Omega \cdot \text{cm}^2)$	$C_{OF}/(\mu\text{F} \cdot \text{cm}^{-2})$	$R_{OF}/(\Omega \cdot \text{cm}^2)$
		$C_{LDH}/(\times 10^{-6} \mu\text{F} \cdot \text{cm}^{-2})$	α_{LDH}			
1	21.76	9.0114	0.8055	3582	0.11346	4065
3	27.02	17.168	0.7431	1574	0.01193	2711
6	26.64	5.4622	0.7619	1071	4.8145×10^{-4}	2985
12	19.18	5.0267	0.6956	9238	5.9551×10^{-4}	9016
24	26.66	8.5164	0.7550	5793	5.1768×10^{-4}	3955

2.3 Growth behaviors of the LDH films

From the data presented in Fig.1, Fig.2 and Fig.3, it is possible to verify a general tendency of the Mg-Al LDH grains sizes to increase for longer time of reaction^[34]. Not only the increase in the Mg-Al LDH content in the composite film, but also the increase in the thickness and denseness of the film were the important factors for improving the corrosion resistance^[4]. However, for the corrosion resistance of the samples obtained with 24 h reaction began to decrease. This suggested two competitive behaviors affecting the crystal growth during the reaction, consistent with the Ostwald ripening phenomenon^[35-36]: dissolution and recrystallization. As showed in Fig.6, the growth process can be distributed to three stages. First stage, some small LDH grains grow at the surface randomly (contrast to the specimens reacted for 1 h, 3 h, 6 h). The LDH film can not cut off the connections between the solution and the substrate efficiently. Second stage, with the reaction

time extending, large amounts of LDH grains cover the anodic oxide film absolutely (contrast to the specimens reacted for 12 h). As shown in Fig.1, the entire surface is covered by LDHs nano-sheets, and some sphere-like structures, which is energetically favorable, as it reduces the strain energy in the crystals. Both thickness and crystal size of LDH films increase with time^[37]. This result is consistent with results of the previous works^[38-39]. Third stage, the size of the LDH grains increased, but the density of the film decreased (contrast to the specimens reacted for 24 h). The reaction time was too long that some tiny LDH grains were dissolved by the solution but the bigger LDH grains continued to grow and the bigger grain stretched the gap between the LDH grains, and solution penetrated into the film through the gap of the LDH sheet. However, as the time extended, the thickness of the film layer increased, and the solution is prevented from contacting the substrate. So the corrosion resistance increased.

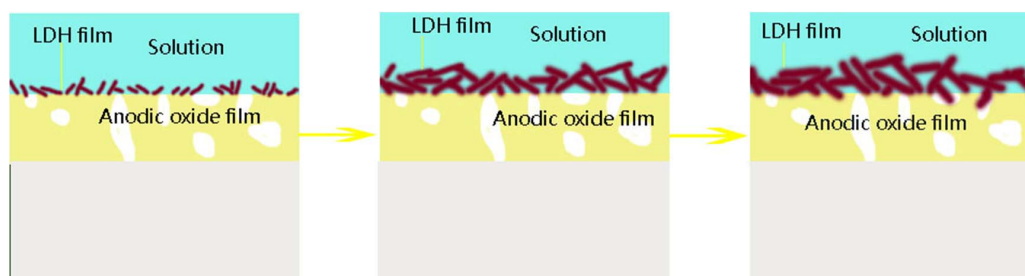


Fig.6 Growth behaviors of the LDH film

3 Conclusions

In this study, the effect of reaction time on growth behaviours of Mg-Al LDH films are studied. The main conclusions are obtained through experiments and characterization analysis as following:

The reaction time affects the crystallinity and grain size. Then the grain size and the morphology of LDH film could be controlled effectively by changing the reaction time that is the realization of controllable preparation of LDH based thin film materials.

Prolonging the reaction time can increase the density of the film greatly, and the samples reacted for 12 h have the best corrosion resistance. When the reaction time is more than 12 h, the LDH film could seal the

pores of anodic oxide film completely to achieve a good sealing effect.

The corrosion resistance of the Mg-Al LDH decreased after 12 h reaction. This maybe explained by that some small LDH grains were dissolved by the solution and the increasing of the grain size stretched the gap between the LDH grains. Then the LDH film cannot inhibit the contact of a magnesium oxide film surface with corrosive medium.

Reference

- [1] ZHANG F, ZHAO L, CHEN H, et al. Corrosion resistance

- of superhydrophobic layered double hydroxide films on aluminum[J]. *Acta metallurgica sinica*, 2010, 47(13): 2466-2469.
- [2] NINLACHART J, RAJA K S. Threshold chloride concentration for passivity breakdown of Mg-Zn-Gd-Nd-Zr alloy (EV31A) in basic solution[J]. *Acta metallurgica sinica (english letters)*, 2017, 30(4): 352-366.
- [3] JIANG Y, TANG G, SHEK C, et al. Effect of electropulsing treatment on microstructure and tensile fracture behavior of aged Mg-9Al-1Zn alloy strip[J]. *Applied physics A: Materials science & processing*, 2009, 97(3): 607-615.
- [4] KAMIYAMA N, PANOMSUWAN G, YAMAMOTO E, et al. Effect of treatment time in the Mg(OH)₂/Mg-Al LDH composite film formed on Mg alloy AZ31 by steam coating on the corrosion resistance[J]. *Surface & coatings technology*, 2016, 286(7): 172-177.
- [5] NAVARRO D R D, CRUZ L R, de CAMPOS J B, et al. Mg substituted apatite coating from alkali conversion of acidic calcium phosphate[J]. *Materials science & engineering C: Materials for biological applications*, 2017, 70(1): 408-417.
- [6] KATO K, TSUZUKI A, TORII Y, et al. Morphology of thin anatase coatings prepared from alkoxide solutions containing organic polymer, affecting the photocatalytic decomposition of aqueous acetic acid[J]. *Journal of materials science*, 1995, 30(3): 837-841.
- [7] RAMEZANI M G, DEMKOWICZ M J, FENG G, et al. Joining of physical vapor-deposited metal nano-layered composites[J]. *Scripta materialia*, 2017, 139(7): 114-118.
- [8] LEE J, JUNG U, KIM W, et al. Effects of residual water in the pores of aluminum anodic oxide layers prior to sealing on corrosion resistance[J]. *Applied surface science*, 2013, 283(11): 941-946.
- [9] GU C D, YAN W, ZHANG J, et al. Corrosion resistance of AZ31B magnesium alloy with a conversion coating produced from a choline chloride: Urea based deep eutectic solvent[J]. *Corrosion science*, 2016, 106(5): 108-116.
- [10] WANG S, PENG H, SHAO Z, et al. Sealing of anodized aluminum with phytic acid solution[J]. *Surface & coatings technology*, 2016, 286: 155-164.
- [11] FRANCIS R C, ANDREAS L, WAGENKNECHT U, et al. Intercalation of Mg-Al layered double hydroxide by anionic surfactants: Preparation and characterization[J]. *Applied clay science*, 2008, 38(3-4): 153-164.
- [12] LIN J K, UAN J Y, WU C P, et al. Direct growth of oriented Mg-Fe layered double hydroxide (LDH) on pure Mg substrates and in vitro corrosion and cell adhesion testing of LDH-coated Mg samples[J]. *Journal of materials chemistry*, 2011, 21(13): 5011-5020.
- [13] HIRAHARA H, AISAWA S, AKIYAMA T, et al. Intercalation of polyhydric alcohols into Mg-Al layered double hydroxide by calcination-rehydration reaction[J]. *Clay science*, 2008, 13: 27-34.
- [14] DASGUPTA S. Controlled release of ibuprofen using MgAl-LDH nano carrier[J]. *IOP conference series: Materials science and engineering*, 2017, 225: 012005.
- [15] GUO X, ZHANG F, EVANS D G, et al. Layered double hydroxide films: Synthesis, properties and applications[J]. *Chemical communications*, 2010, 46(29): 5197-5210.
- [16] HE S, ZHAO Y F, WEI M, et al. Preparation of oriented layered double hydroxide film using electrophoretic deposition and its application in water treatment[J]. *Industrial & engineering chemistry research*, 2011, 50(5): 2800-2806.
- [17] VEGA J M, GRANIZO N, FUENTE D D L, et al. Corrosion inhibition of aluminum by coatings formulated with Al-Zn-vanadate hydrotalcite[J]. *Progress in organic coatings*, 2011, 70(4): 213-219.
- [18] ZHANG F, SUN M, XU S, et al. Fabrication of oriented layered double hydroxide films by spin coating and their use in corrosion protection[J]. *Chemical engineering journal*, 2008, 141(1): 362-367.
- [19] TAMÁS A, VIKTÓRIA H, IMRE D. Layered double hydroxides for ultrathin hybrid film preparation using layer-by-layer and spin coating methods[J]. *Colloids & surfaces A: Physicochemical & engineering aspects*, 2008, 319(1): 116-121.
- [20] HAN J, XU X, RAO X, et al. Layer-by-layer assembly of layered double hydroxide/cobalt phthalocyanine ultrathin film and its application for sensors[J]. *Journal of materials chemistry*, 2011, 21: 165.
- [21] ZHANG F, ZHANG C L, SONG L, et al. Corrosion of in-situ grown MgAl-LDH coating on aluminum alloy[J]. *Transactions of Nonferrous Metals Society of China*, 2015, 25(10): 3498-3504.
- [22] ZHOU M, PANG X, WEI L, et al. Insitu grown superhydrophobic Zn-Al layered double hydroxides films on magnesium alloy to improve corrosion properties[J]. *Applied surface science*, 2015, 337: 172-177.
- [23] TEDIM J, POZNYAK S K, KUZNETSOVA A, et al. Enhancement of active corrosion protection via combination of inhibitor-loaded nanocontainers. [J]. *ACS applied materials & interfaces*, 2010, 2(5): 1528.
- [24] ISHIZAKI T, KAMIYAMA N, WATANABE K, et al. Corrosion resistance of Mg(OH)₂/Mg-Al layered double hydroxide composite film formed directly on combustion-resistant magnesium alloy AMCa602 by steam coating[J]. *Corrosion science*, 2015, 92: 76-84.
- [25] TEDIM J, BASTOS A C, KALLIP S, et al. Corrosion protection of AA2024-T3 by LDH conversion films[J]. *Electrochimica acta*, 2016, 210: 215-224.
- [26] ZHOU M, PANG X, WEI L, et al. Insitu grown superhydrophobic Zn-Al layered double hydroxides films on magnesium alloy to improve corrosion properties[J]. *Applied surface science*, 2015, 337: 172-177.
- [27] KUZNETSOV B, SERDECHNOVA M, TEDIM J, et al. Sealing of tartaric sulfuric (TSA) anodized AA2024 with

- nanostructured LDH layers[J]. RSC advances, 2016, 17 (6): 13942-13952.
- [28] ZHANG F, LIU Z G, ZENG R C, et al. Corrosion resistance of MgAl-LDH coating on magnesium alloy AZ31 [J]. Surface & coatings technology, 2014, 258: 1152-1158.
- [29] KAMEDA T, FUBASAMI Y, YOSHIOKA T. Kinetics and equilibrium studies on the treatment of nitric acid with Mg-Al oxide obtained by thermal decomposition of NO_3^- -intercalated Mg-Al layered double hydroxide[J]. Journal of colloid & interface science, 2011, 362(2): 497-502.
- [30] CHEN H, ZHANG F, FU S, et al. In-situ microstructure control of oriented layered double hydroxide monolayer films with curved hexagonal crystals as superhydrophobic materials[J]. Chem inform, 2006, 18(23): 3089-3093.
- [31] LEI C, ZHU X, ZHU B, et al. Superb adsorption capacity of hierarchical calcined Ni/Mg/Al layered double hydroxides for congo red and Cr(VI) ions[J]. Journal of hazardous materials, 2017, 321: 801-811.
- [32] LI Y, LI S, ZHANG Y, et al. Enhanced protective Zn-Al layered double hydroxide film fabricated on anodized 2198 aluminum alloy[J]. Journal of alloys and compounds, 2015, 630: 29-36.
- [33] DING P, LI Z, WANG Q, et al. In-situ growth of layered double hydroxide films under dynamic processes: Influence of metal cations[J]. Materials letters, 2012, 77(12): 1-3.
- [34] XU Z P, STEVENSON G, LU C Q, et al. Dispersion and size control of layered double hydroxide nanoparticles in aqueous solutions[J]. Journal of physical chemistry B, 2006, 110(34): 16923-16929.
- [35] JONES R G, KAHOVEC J, STEPTO R, et al. Definitions of terms relating to the structure and processing of sols, gels, networks and inorganic-organic hybrid materials (2007)[J]. Pure & applied chemistry, 2009, 354: 895.
- [36] GALVÃO T L, NEVES C S, CAETANO A P, et al. Control of crystallite and particle size in the synthesis of layered double hydroxides: Macromolecular insights and a complementary modeling tool[J]. Journal of colloid and interface science, 2016, 468: 86-94.
- [37] ZHANG G, WU L, TANG A T, et al. Growth behavior of MgAl-layered double hydroxide films by conversion of anodic films on magnesium alloy AZ31 and their corrosion protection[J]. Applied surface science, 2018, 456: 419-429.
- [38] ELISEEV A V L A A, VERTEGEL A A, TARASOV V P, et al. A study of crystallization of Mg-Al double hydroxides[J]. Doklady chemistry, 2002, 387: 339-343.
- [39] CHEN H Y, ZHANG F Z, CHEN T, et al. Comparison of the evolution and growth processes of films of M/Al-layered double hydroxides with M=Ni or Zn[J]. Chemical engineering science, 2009, 64: 2617-2622.